Structural Transitions of Myosin Associated with Force Generation in Spin-labeled Muscle Fibers

A DISSERTATION
SUBMITTED TO THE FACULTY OF THE GRADUATE SCHOOL
OF THE UNIVERSITY OF MINNESOTA
BY

Ryan Nicholas Mello

IN PARTIAL FULFILLMENT OF THE REQUIREMENTS
FOR THE DEGREE OF
DOCTOR OF PHILOSOPHY

David D. Thomas, advisor

June 2012

Acknowledgements

There are many people who have provided me with support in one way or another as I completed my PhD. To all of you, I am deeply thankful.

First, I want to acknowledge my advisor **Dr. David Thomas**. Without his support, guidance and encouragement this work would not have been possible. Dr. Thomas is a gifted scientist and leader, and from him I have learned a great deal about science and life. Dr. Thomas is a living example of “do what you love, and love what you do.”

I also want to thank my committee members: **Dr. Dawn Lowe**, **Dr. Vincent Barnett** and **Dr. Russell Ritenour**. They have provided invaluable instruction in my graduate courses an guidance as I progressed through graduate school.

Octavian Cornea and **Sarah Blakely**, I am not sure what I would have done without you two. Over the past six years the two of you have had the answer to literally every question I have asked of you. Your expertise has saved me countless hours. Thank you for your knowledge and friendship.

I want to extend a special thanks to the senior graduate students, now postdoctoral fellows, who taught me the practical aspects of being a biophysicist and a graduate student: **Dr. David Kast**, **Dr. Andrew Thompson** and **Dr. Roman Agafonov**. Outside the lab, Dave Kast was always primed to have fun, Andrew’s wit was always entertaining and Roman’s constant question “Why?” always kept me on my toes.

Over the past six years I have been fortunate to have outstanding technical support in areas where my knowledge was lacking. **Florentin Nitu**, **Leanne Kolb** (now Anderson), **Eunice Song**, **Christina Yi**, **Evan Smith, Edmund Howard** and **Tyler**

Miller, I am grateful for your assistance. I have also had the opportunity to work with some talented and motivated undergraduates, **Bobby Harris** and **Doug Deitchler**.

Thank you **Jesse McCaffrey** and **Zach James** for insightful conversations about EPR spectroscopy. Thanks **John Rubin** and **Yun Lin** for helping my pursuit of a career in medicine; maybe we will work together in the clinic someday. And thank you **Becca Moen**, **Ben Binder**, **Karl Petersen** and **Dr. Bengt Svensson** for all the help with the BSL project.

I also need to thank my in-laws. **Rick** and **Jean Bearden** have shown me unconditional love and support and provided countless meals. Thank you **Camille Bearden** for all the fun times you have spent with me and Caili, and your priceless Kristen Wiig impressions. Thanks **Alex Bearden** for making me laugh uncontrollably, and thank you **Meredith Bearden** for being quite possibly the sweetest person on earth. And **Patty Bearden**, thanks for keeping life interesting with your attitude. You are all very important in my life.

And finally, I need to thank my extended family for providing love, support, and fun over the past 28 years. **Grandpa** and **Grandma Skatrud**, you have shaped my life since the moment I was born and still touch my life to this day. **Grandpa** and **Grandma Mello**, you are missed greatly and your love will always be with me. **David Skatrud**, **John Skatrud**, **Kari** and **Matt McCreedy** and **John** and **Cheri Mello,** I can't thank you enough for all the joy you have brought into my life (Duke basketball games, skiing, ping-pong, inspiration, beer…the list goes on). **Caili**, **Danielle**, **Frank** and **Mary**, this is for you (next page).

Dedication

To my wife, ***Caili Mello***
"If I know what love is, it is because of you" ~ Hermann Hesse

And

To my parents and sister, ***Frank, Mary and Danielle Mello***
"Be brave. Take risks. Nothing can substitute experience." ~ Paulo Coelho

Abstract

Muscle contraction is driven by the actin-activated hydrolysis of ATP by myosin, resulting in the relative sliding of actin and myosin filaments. Current models propose that filament sliding is driven by a structural transition of myosin's catalytic domain (CD) and light chain domain (LCD). The goal of this research is to measure structural transitions of myosin II (muscle and nonmuscle) that are associated for force generation. Structural measurements were made using electron paramagnetic resonance (EPR) spectroscopy. This work is comprised of two separate, but related, projects.

In the first project (Chapter 3), thiol crosslinking and EPR were used to resolve structural transitions of myosin's LCD and CD that are associated with force generation. Spin labels were incorporated into the LCD of muscle fibers by exchanging spin-labeled regulatory light chain (RLC) for endogenous RLC, with full retention of function. LCD orientation and dynamics were measured in three biochemical states: relaxation (A.M.T), post-hydrolysis intermediate (A.M′.D.P), and rigor (A.M.D). To trap myosin in a structural state analogous to the elusive post-hydrolysis ternary complex A.M′.D.P, we used pPDM to crosslink SH1 (Cys707) to SH2 (Cys697) on the CD. EPR showed that the LCD of crosslinked fibers has an orientational distribution intermediate between relaxation and rigor, and saturation transfer EPR revealed slow rotational dynamics indistinguishable from that of rigor. Similar results were obtained for the CD using a bifunctional spin label to crosslink SH1 to SH2, but the CD was more disordered than the LCD. We conclude that SH1-SH2 crosslinking traps a state in which both the LCD and CD are in a structural state intermediate between relaxation (highly disordered and

microsecond dynamics) and rigor (highly ordered and rigid), supporting the hypothesis that the crosslinked state is an A.M′.D.P analog on the force generation pathway.

In the second project, we present a method for obtaining high-resolution structural information of proteins using EPR of a bifunctional spin label (BSL). Two complimentary EPR techniques were employed to measure dynamics and orientation (conventional EPR) and intraprotein distances (dipolar electron-electron resonance). The exploitation of BSL is a key feature of this work. BSL attaches at residue positions *i* and *i*+4, which drastically restricts probe motion compared to monofunctional probes. For comparison, measurements were also made with the monofunctional spin label MSL. Subfragment 1 of *Dictyostelium* myosin II (S1dC) was used to exemplify the increased resolution provided by BSL. Using this approach, we demonstrate with experiments that BSL significantly increases resolution when measuring distance and orientation compared to MSL. And while this work does focus on the methodology, there is significant biological insight into myosin's nucleotide-dependent structural transitions.

Table of Contents

ACKNOWLEDGEMENTS ..... **I**

DEDICATION ..... **III**

ABSTRACT ..... **IV**

LIST OF TABLES ..... **VII**

LIST OF FIGURES ..... **VIII**

ABBREVIATIONS ..... **X**

CHAPTER 1: INTRODUCTION TO MUSCLE CONTRACTION & MYOSIN **1**

1.1 Skeletal Muscle Contraction 1
1.2 Myosin Structure 4
1.3 The Actomyosin ATPase Cycle 5
1.4 Motivation for Research 7

CHAPTER 2: ELECTRON PARAMAGNETIC RESONANCE **9**

2.1 Angular Momentum and Spin 9
2.2 The Zeeman Effect 10
2.3 The EPR spectrometer 13
2.4 Site-Directed Spin Labeling 14
2.5 Nuclear Hyperfine Interaction 15
2.6 EPR is Sensitive to Orientation 17
2.7 EPR is sensitive to Dynamics 19
2.7.1 Conventional EPR *20*
2.7.2 Saturation Transfer EPR (STEPR) *22*
2.8 Fitting EPR Spectra 23

CHAPTER 3: THREE DISTINCT ACTIN-ATTACHED STRUCTURAL STATES OF MYOSIN IN MUSCLE FIBERS **26**

3.1 Overview 27
3.2 Introduction 27
3.3 Methods 32
3.4 Results 36
3.5 Discussion 44
3.6 Supplementary Material 51
3.7 Future Directions 62

CHAPTER 4: A HIGH-RESOLUTION EPR TECHNIQUE FOR MEASURING PROTEIN STRUCTURAL DYNAMICS **67**

4.1 Overview 67
4.2 Introduction 68
4.3 Methods 72
4.4 Results 77
4.5 Discussion 83
4.6 Future Directions 88

BIBLIOGRAPHY **91**

List of Tables

Table 1 ATPase assays..... 37
Table 2 Distance distributions 83

List of Figures

Figure 1 Skeletal muscle structure. 2
Figure 2 The contracting sarcomere. 3
Figure 3 Myosin Structure. 5
Figure 4 The actomyosin ATPase cycle. 6
Figure 5 The Zeeman Effect. 11
Figure 6 The basics of an EPR spectrometer. 13
Figure 7 Nitroxide spin labels. 14
Figure 8 The Hyperfine Interaction. 16
Figure 9 Orientation of the applied magnetic field in the spin label coordinate frame. .. 17
Figure 10 Sensitivity of EPR to orientation. 18
Figure 11 Dynamics, conventional EPR. 21
Figure 12 Dynamics, saturation transfer EPR. 23
Figure 13 Model for coupling of actomyosin ATPase to force and movement. 30
Figure 14 Conventional EPR spectra (V_1) of spin-labeled LCD. 39
Figure 15 Structural models based on EPR spectra. 40
Figure 16 Effect of pPDM crosslinking on EPR spectra of spin-labeled myosin LCD. . 42
Figure 17 EPR spectra of skinned fiber bundles labeled on myosin CD with BSL. 43
Figure. 18 Updated model for coupling of actomyosin ATPase to force. 51
Figure 19 Improved RLC exchange. 54
Figure 20 Extent of RLC exchange. 57
Figure 21 Sensitivity of conventional EPR to orientational distributions. 60
Figure 22 Dependence of EPR spectra on isotropic rotational correlation time. 61
Figure 23 FDNASL vs. BSL on the RLC in psoas fibers. 63
Figure 24 Wobble in a cone. 64
Figure 25 Blebbistatin 66
Figure 26 BSL, MSL and Dictyostelium *discoideum* myosin II catalytic domain. 71
Figure 27 BSL and MSL minced spectra. 78
Figure 28 BSL and MSL oriented spectra. 80

Figure 29 BSL and MSL DEER and distance distributions. 82
Figure 30 S1dC labeling sites and 639.643 spectra. 88

Abbreviations

A, actin

ADP or D, adenosine diphosphate

ATP or T, adenosine triphosphate

BSL, 3,4-bis-(methanethiosulfonyl-methyl)-2,2,5,5-tetramethyl-2,5-dihydro-1h-pyrrol-1-yloxy

CD, myosin catalytic domain

Cys, cysteine

LCD, myosin light chain domain

M, myosin

MSL, N-(1-oxy-2,2,6,6-tetramethyl-4-piperidinyl)maleimide.

P or P_i , inorganic phosphate

pPDM, N,N′-(1,4-phenylene)dimaleimide

S1dC, subfragment 1 of *Dictyostelium discoideum* myosin II

Tn, troponin

Chapter 1: Introduction to Muscle Contraction & Myosin

Many processes that are essential to the existence of living organisms require self-propelled movement. Examples include chromosome separation during cell division, molecular transport within cells, the beating action of a heart and the inhalation of fresh air into lungs. The powerhouses for these forms of movement, and many others, are a group of biological macromolecules known as motor proteins. Motor proteins use energy derived from ATP hydrolysis to do mechanical work. There are three types of motor proteins: kinesin, dynein and myosin. This work is focused on myosin, specifically myosin II (which includes muscle myosin).

1.1 Skeletal Muscle Contraction

Muscle contraction is an intricate process requiring precise coordination of neurotransmitters, ions, nucleotides, and proteins. To investigate skeletal muscle contraction on a molecular level, it is important to first examine muscle structure from a macroscopic to microscopic scale (**Figure 1**). Moving from the gross visualization of muscle tissue, the first subunit is the fascicle which is composed of a parallel bundle of muscle cells (also referred to as muscle fibers). Each muscle fiber contains several myofibrils, and each myofibril is made of several sarcomeres. The sarcomere is the organelle within the muscle cell that is responsible for movement (1). Each sarcomere contains an interdigitating lattice of myosin and actin filaments, known as the thick (myosin) and thin (actin) filaments. Muscle contraction is driven by the actin-activated

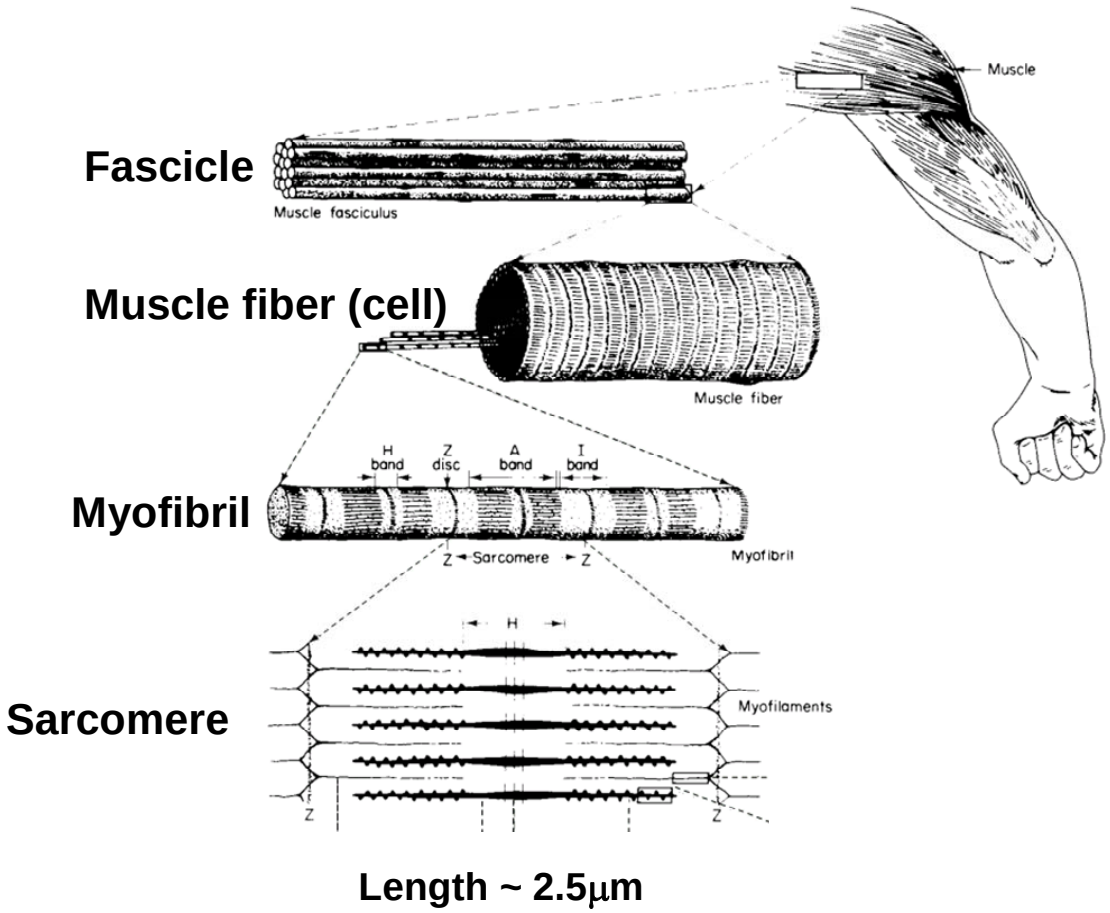

Figure 1 Skeletal muscle structure.
Adapted from Bloom and Fawcett, *Textbook of Histology*, 11th ed. Philadelphia, WB Saunders, 1986 page 282.

hydrolysis of ATP by myosin, resulting in the relative sliding of actin and myosin filaments (**Figure 2**).

Myosin is the molecular motor driving muscle contraction, however, force production involves several other contractile proteins. As mentioned above, the primary component of the thin filament is actin. Actin is a 43kD protein that myosin binds during muscle contraction. Under physiological conditions, actin polymerizes to form an α-helical double-stranded filament. The proteins troponin and tropomyosin bind to the actin filament backbone, and aid in the Ca^{2+} regulation of skeletal muscle contraction.

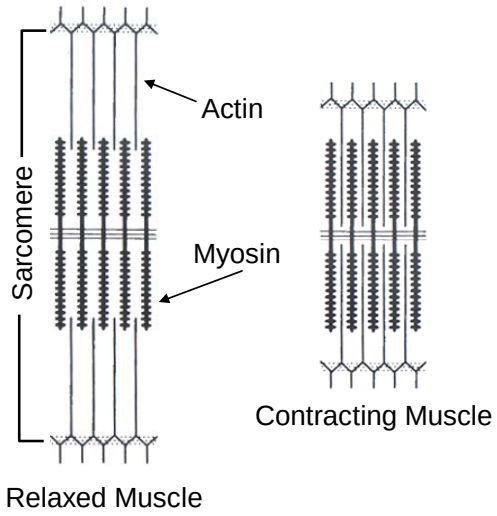

Figure 2 The contracting sarcomere.
Schematic representation of the fundamental unit of muscle contraction, the sarcomere, emphasizing the relative sliding of actin and myosin filaments during contraction. The sarcomere is composed of interdigitating myosin (thick) and actin (thin) filaments. Adapted from (1).

Tropomyosin is a 65 kDa protein that forms an α-helical dimer and binds to the actin filament. Troponin (Tn) is a three subunit complex consisting of TnC (18 kDa), TnT (30 kDa) and TnI (30 kDa). The Tn complex binds Ca^{2+} and controls the conformation of tropomyosin on actin. During relaxation, cytosolic Ca^{2+} is low (~ 0.1 μM), and tropomyosin is locked over the myosin biding site on actin. During contraction, the sarcoplasmic reticulum releases Ca^{2+}, increasing the cytoplasmic Ca^{2+} to ~ 10 μM. TnC then binds Ca^{2+} and undergoes a conformational change. This conformational change is relayed to TnT and TnI. TnI then unlocks tropomyosin from the myosin binding site, enabling myosin to bind actin.

In addition to those mentioned above, there are other proteins associated with the thick (myosin) and thin (actin) filaments. Titin is a massive protein (MW greater than 3 MDa) that contributes to muscle assembly, resting tension and sarcomere length (2). Myosin-Binding protein-C (c-protein) contributes to the formation and stabilization of

thick filaments and is thought to modulate contractility by interacting with both thick and thin filaments (3). Nebulin is associated with the thin filament, and is thought to play a role in the regulation of thin filament length and muscle contractility (4). There are additional proteins within the sarcomere, but the ones mentioned above are those predominantly associated with the thick and thin filaments.

Muscle contraction is produced by the actin-activated hydrolysis of ATP by myosin (5). This results in the relative sliding of actin and myosin filaments (**Figure 2**). Mechanistic models propose that filament sliding is driven by a structural transition of the myosin catalytic domain (CD) from a dynamically disordered state of weak actin binding to an ordered state of strong actin binding, and a lever arm rotation of the light-chain domain (LCD)(6-9). This work presented herein focuses on these force-generating structural transitions of myosin.

1.2 Myosin Structure

Myosin is a dimeric protein with a molecular weight of approximately 500kD. Each protomer contains a 120 kDa head and a long α-helical C-terminal tail. The two tails bind to form a coiled coil, which unites the two heads (**Figure 3**, top). The myosin head (which can be isolated proteolytically as subfragment 1, or S1) consists of the N-terminal catalytic domain (CD) and the light-chain domain (LCD) (**Figure 3**, bottom). The CD contains the ATP-binding pocket and the actin-binding region. The LCD contains a single α-helix, extending C-terminally from the CD, to which are bound two light chains, the essential light chain (ECL) and the regulatory light chain (RLC).

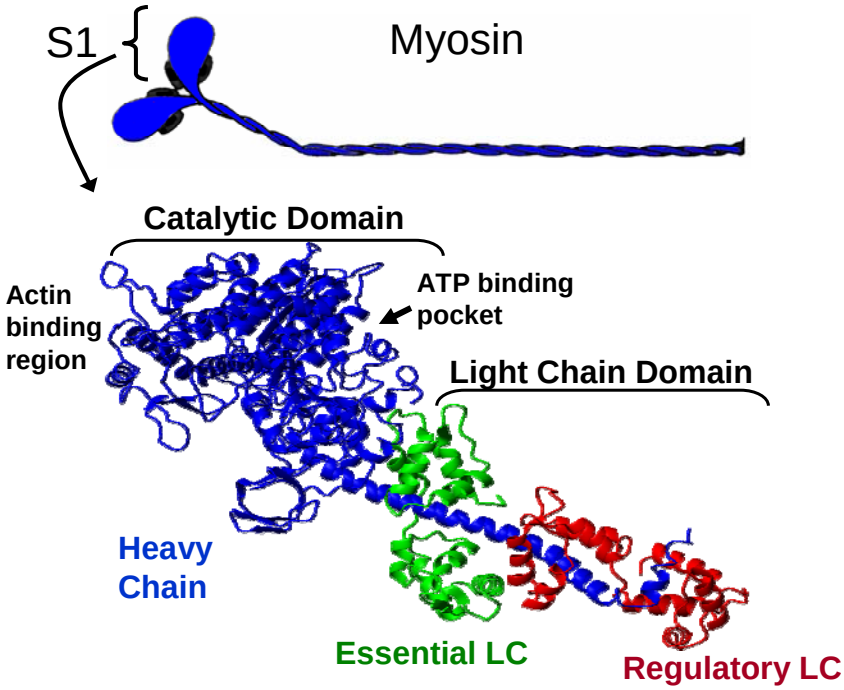

Figure 3 Myosin Structure.
Top: Cartoon illustrating the dimeric myosin molecule including the long α-helical tale and two heads. Bottom: Crystal structure of the myosin head (S1) (10). The catalytic domain contains the actin binding region and the ATP binding pocket. The two light chains are shown in green (essential light chain) and red (regulatory light chain).

1.3 The Actomyosin ATPase Cycle

During ATPase cycling, the interaction between myosin and actin can be classified (to a first approximation) as either weak, when ATP is bound to myosin, or strong, when ADP or no nucleotide is bound (11). Mechanistic models propose that force generation in muscle is driven by a structural transition of the myosin catalytic domain (CD) from a dynamically disordered state of weak actin binding to an ordered state of strong actin binding, and a lever arm rotation of the light-chain domain (LCD)(6-10).

A schematic model demonstrating the actomyosin ATPase is shown in **Figure 4**. This model (adapted from (12)) focuses on the coupling between myosin's force-producing structural transitions (based on crystal structures (13,14) and spectroscopy (11)) and biochemical state (defined by the active site ligand) and actin binding properties of myosin. The post-powerstroke rigor state (**Figure 4**, A) is populated when myosin is in apo or ADP biochemical states. In rigor myosin has a strong actin affinity (K_d < 1 μM) and the CD is well oriented on actin with slow (ms) dynamics. After ADP release, ATP binding (**Figure 4**, B) weakens the actin-myosin interaction, dissociating actin from myosin (relaxation). In relaxation myosin has a weak affinity for actin (K_d =

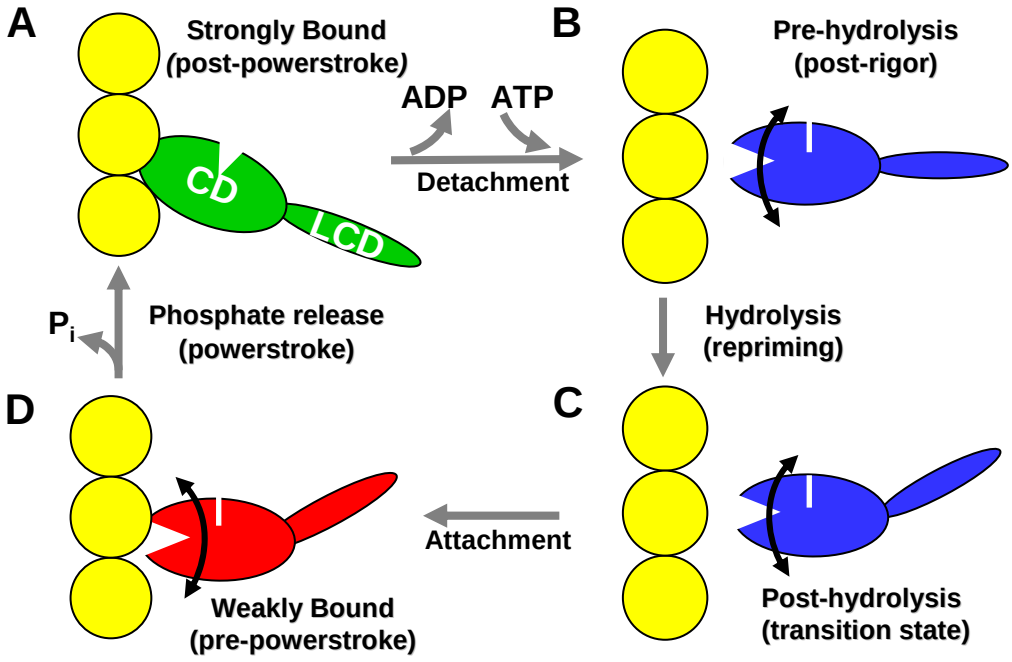

Figure 4 The actomyosin ATPase cycle.
Proposed structural changes of myosin S1 during ATPase cycling. This model focuses on the coupling between the force-producing structural changes and myosin's biochemical state (defined by the active site ligand) and actin binding properties. Adapted from (12).

100 μM) and the CD is dynamically disordered (μs dynamics). Myosin then hydrolyzes ATP to ADP.P_i, and undergoes a repriming (**Figure 4**, B-C). Next, the post-hydrolysis complex forms a weak binding complex with actin (**Figure 4**, C-D) (5), and there is evidence that force generation begins in this biochemical state, before phosphate is released but after isomerization (**Figure 4**, C-D) (15,16). The powerstroke is then completed as P_i is released, and myosin undergoes a force producing weak-to-strong transition (also referred to as a disorder-to-order transition) (**Figure 4**, D-A).

1.4 Motivation for Research

For several reasons, the structure of muscle (particularly striated muscle) has made the muscle fiber an attractive system for investigating movement in living organisms (12). First, the primary proteins involved in muscle contraction, actin and myosin, comprise 80% of the structural proteins present within the cell, enabling the isolation of relatively large amounts of these proteins for characterization. Second, the contractile organelle, the sarcomere, is highly organized and repetitive. Such organization has made it possible to deduce structural information, on the molecular level, from x-ray diffraction and microscopy. Third, muscle contraction is macroscopic. Unidirectional shortening of muscle has made it possible to characterize the mechanical properties of muscle such as length, force and velocity. The results, models and theories discussed in sections 1.1 – 1.3 represents a small subset of the research done to understand muscle contraction on a molecular level. Several disciplines, including biochemistry, physiology, microscopy, crystallography, and spectroscopy, have contributed to the understanding of

muscle contraction on the molecular level. These techniques and theories have also been applied to the study of the other molecular motors, kinesin and dynein.

In this work, we used electron paramagnetic resonance spectroscopy (EPR) to investigate muscle contraction on a molecular level. EPR is an ideal tool for studying a dynamic process such as muscle contraction because it is sensitive to both orientation and dynamics (sections 2.6 and 2.7). Measurements using spin-labeled myosin (a spin label is a small organic molecule with a stable unpaired electron) were made with myosin bound to actin in oriented muscle fiber bundles. Therefore, unlike solution work where myosin is tumbling isotropically, we were able to orientate myosin using the intrinsic order of the muscle fiber. Fiber bundles were oriented with the long axis parallel or perpendicular to the applied magnetic field (H), making it possible to measure changes in myosin orientation relative to the actin filament axis. Spectra were acquired while perfusing the fiber bundle with solution, making it possible to change the biochemical state of the muscle during acquisition. Chapter 3 and 4 summarize this work, and demonstrate the power of this approach for making high resolution structural measurements of myosin in the presence of actin. Structural measurements were made in several biochemical states, but special emphasis was placed on myosin's structural transitions that initiate force generation (**Figure 4**, D-A). These post-hydrolysis early-force complexes have remained elusive and difficult to study because actin (i) greatly accelerates the rate of P_i release, and (ii) shifts the equilibrium constant for hydrolysis toward the prehydrolysis state by a factor of 20 (17).

Chapter 2: Electron Paramagnetic Resonance

Electron Paramagnetic resonance is a technique capable of detecting unpaired electrons. When an unpaired electron is placed in strong magnetic field, incident microwaves may be absorbed causing electron-spin reorientation (18). The EPR spectrum can then be used to characterize the g-factor for the sample.

$$g = \frac{h\nu}{\beta H_0}$$

The g-factor is a measure of the local magnetic field experienced by the electron, and it is a characteristic quantity of electron environment. Additionally, the observed g-factor is often anisotropic, that is, its value is dependent on the orientation of the molecule in the magnetic field (18). Consequently, EPR is useful for not only detecting unpaired electrons, but for gaining insight about the electron's environment, orientation, and dynamics. In this work, EPR was used to measure myosin orientation and dynamics. The remainder of Chapter 2 covers the basic principles of EPR spectroscopy, and its application to measuring myosin orientation and dynamics.

2.1 Angular Momentum and Spin

In classical mechanics, a rigid body possesses two kinds of angular momentum; (a) orbital angular momentum (**L** = **r** x **p, r** is the position vector relative or origin and **p** is the momentum) associated with the motion of the center of mass and (b) spin angular momentum (**S** = ***I*****ω**, ***I*** is the moment of inertia and **ω** is angular velocity) associated with

motion about the center of mass (19). Similar to the earth revolving around the sun and rotating about its axis, electrons posses orbital and spin angular momentum. For electrons, the orbital angular momentum is associated with motion around the atomic nucleus. However, the spin angular momentum of an electron has nothing to do with its motion in space, even though the spin angular momentum of an electron is often compared to the classical notion of spin. This comparison is a useful tool conceptually, but it fails to describe reality because electrons are believed to be structureless point particles (19). Considering this ambiguous nature of electrons, it is reasonable to say that electrons have an intrinsic spin angular momentum (**S**), though not in a classical sense, in edition to their extrinsic orbital angular momentum (**L**). The spin angular momentum **S** can be described by the spin quantum number m_s, where $m_s = \pm ½$. Just as nuclear magnetic resonance spectroscopy and magnetic resonance imaging manipulate spin states of protons and neutrons, electron paramagnetic resonance manipulates the spin states of electrons.

2.2 The Zeeman Effect

Magnetic resonance refers to the absorption of a photon causing spin to reorient, or flip. In EPR it is the electron spin that flips after absorbing a photon, but only in the presence of a strong magnetic field. In the presence of a magnetic field, the degeneracy of the spin states is broken. That is, in the absence of a magnetic field , ΔE between spin states is 0. In the presence of a magnetic field **H**, ΔE is nonzero. This phenomenon is known as the Zeeman Effect (**Figure 5**), and is explained below.

The magnetic moment of an electron is

$$\boldsymbol{\mu} = \gamma \mathbf{S}$$

where γ is the gyromagnetic ratio (-1.76 x 10^7 rad/(s*G) for an electron) and **S** is the spin angular momentum. The energy of a magnetic moment is a function of the magnetic moment $\boldsymbol{\mu}$ and the magnetic field **H**. If the magnetic field is oriented along the z-axis, the energy can be expressed as

$$E = -\boldsymbol{\mu} \bullet \mathbf{H} = -\gamma \mathbf{S} \bullet \mathbf{H} = -\gamma S_z \bullet H$$

S_z can only have values of $m_s\hbar$, so

$$E = -\gamma m_s \hbar H$$

The gyromagnetic ratio γ is expressed as $-g\beta/\hbar$, therefore

$$E = m_s g \beta H$$

Now, in the presence of an applied magnetic field, there are two energy levels

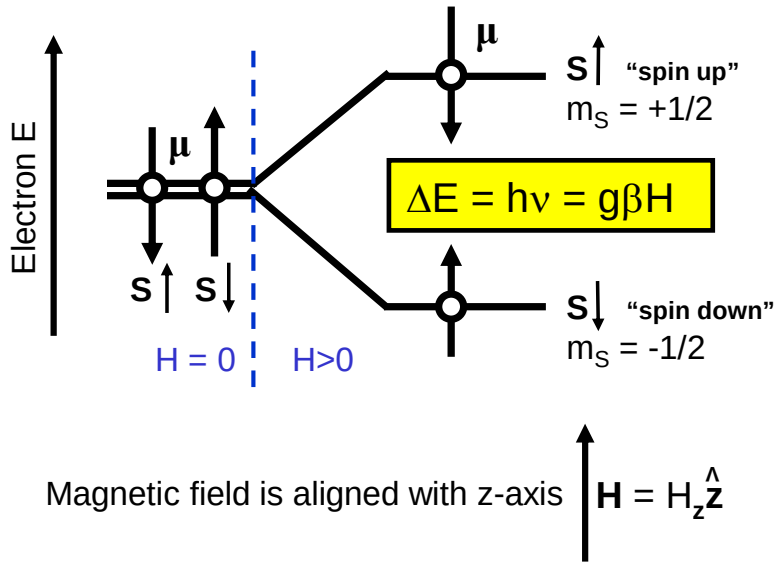

Figure 5 The Zeeman Effect.
Electron energy level splitting in a magnetic field due to the Zeeman Effect. Magnetic resonance occurs when electromagnetic radiation of the appropriate energy is applied perpendicular to the external magnetic field H. Adapted from (18).

corresponding to the two spin states:

$$m_s = + ½ \text{ “spin up”: } E = (½)g\beta H$$

$$m_s = - ½ \text{ “spin down”: } E = (-½)g\beta H$$

Therefore, the energy difference between the two spin states is

$$\Delta E = E_{up} - E_{down} = g\beta H$$

In EPR spectroscopy, magnetic resonance occurs when the microwave energy ($h\nu$) equals ΔE (eq. 2.1, **Figure 5**), which is referred to as the resonance condition

$$h\nu = g\beta H \qquad \textbf{[eq. 2.1]}$$

2.3 The EPR spectrometer

A schematic showing the basic components of an EPR spectrometer is shown in **Figure 6**. In it simplest form, an EPR spectrometer consists of a magnet, a photon (microwave) source, and a resonant cavity. The magnetic field is supplied by an electromagnet. For X-band EPR (used in this work), the microwave frequency is ~ 9.5 GHz, and is supplied by a Gunn Diode. The resonator, where the sample is placed, is called a cavity. The resonance condition (eq. 2.1) can be met by sweeping the magnetic field or the microwave frequency. It is simpler, from an engineering standpoint, to vary the magnetic field strength by varying the current through the electromagnet. Therefore, in EPR spectroscopy the magnetic field is swept while the microwave frequency is held constant. Detection of the absorption signal is improved by modulating the magnetic field,

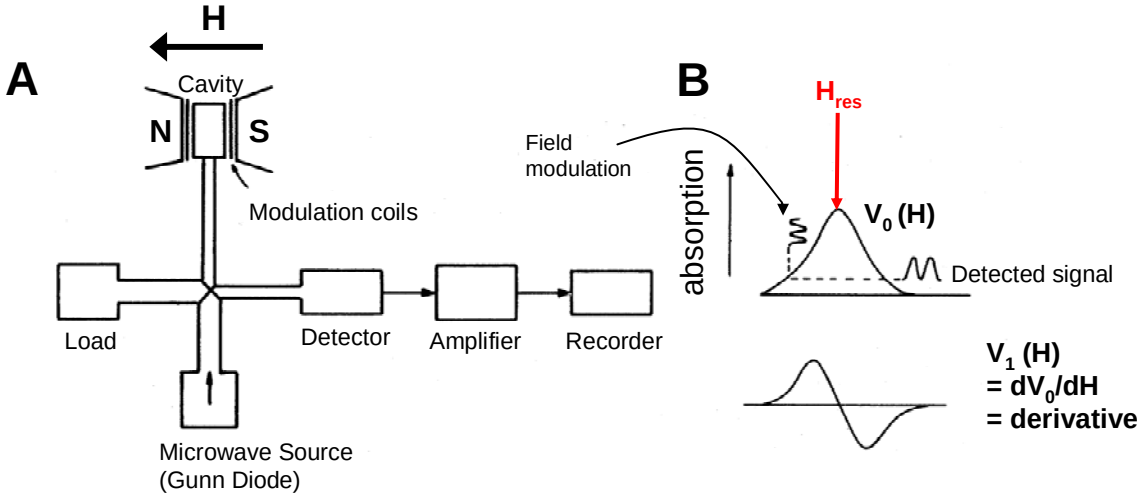

Figure 6 The basics of an EPR spectrometer.
A: Simple schematic highlighting the essential components of an EPR spectrometer. B: EPR spectrum obtained by field modulation and phase-sensitive detection ate the modulation frequency. Adapted from (18).

generally a 100 kHz sinusoidal modulation (18). If this modulation amplitude is less than the linewidth of the absorption signal, and the detector is sensitive to the phase of the signal, the detected signal appears as a derivative of the absorption spectrum (18) (**Figure 6**, B). That is, EPR spectra are viewed as the derivative of absorption (V_1) vs. magnetic field strength (H), rather than absorption (V_0) vs. H.

2.4 Site-Directed Spin Labeling

As explained above, EPR spectroscopy detects unpaired electrons. In biological systems, unpaired electrons occur in some transition metal ions and in free radicals. Free radicals are usually highly reactive and therefore unstable. In order to make structural measurements on myosin, we have used site-directed spin labeling (SDSL). A spin label is a small organic molecule with a stable unpaired electron and the ability to bind to a specific site on another molecule. The unpaired electron is usually on the nitrogen atom in an N-O

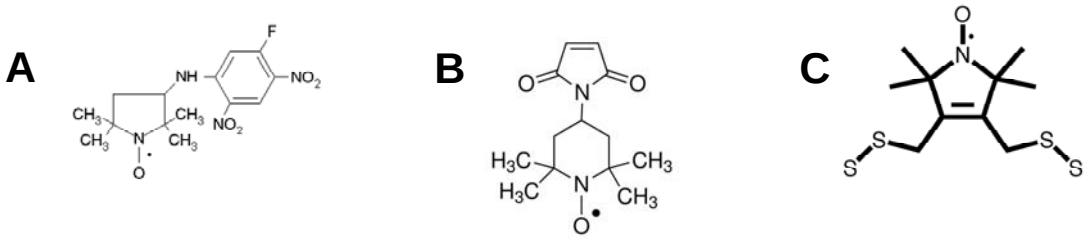

Figure 7 Nitroxide spin labels.
A: 3-(5-f luoro-2,4-dinitroanilino)-2,2,5,5-tetramethyl-1-pyrrolidinyloxy, abbreviated as FDNASL. B: 4-maleimido-2,2,6,6-tetramethyl-1-piperidinyloxy or 4-Maleimido-TEMPO, abbreviated as MSL. C: Trans-3,4-bis-(methanethiosulfonylmethyl)-2,2,5,5-tetramethylpyrrolidin-1-yloxy Radical, abbreviated as BSL.

(nitroxide) bond, hence the name nitroxide spin label. The nitroxide spin labels used in this work (**Figure 7**) bind selectively to the amino acid cysteine (Cys). Given this selectivity, it is possible to attach a spin label to a specific area of interest. Muscle fibers contain several cysteine residues, however strategic labeling conditions makes it possible to selectively label SH1 (Cys707) and/or SH2 (Cys697) on the myosin CD (5). Alternatively, protein engineering can be used to mutate out all reactive Cys residues, and then introduce a labeling site (Cys residue) at resides other than SH1 and SH2 (20,21). In this work, both techniques were used to obtain selective spin-labeling in myosin.

2.5 Nuclear Hyperfine Interaction

With the use of nitroxide spin labels, the hyperfine interaction becomes relevant. The hyperfine interaction is due to the magnetic interaction between the dipole moments of the electron and nearby nuclei. In the case of a nitroxide spin label, it is the magnetic moment of the nitrogen nucleus. Due to the hyperfine interaction, each electron spin state is split into (2I + 1) energy states, where I = nuclear spin. For nitrogen, I = 1, yielding three additional energy states for each electron spin state.

From section 2.2, which describes the Zeeman Effect, the Hamiltonian for an unpaired electron in a magnetic field, neglecting the hyperfine interaction, can be written as

$$\mathcal{H}_{zeeman} = g\beta HS_z/\hbar$$

The hyperfine interaction adds an additional term to the Hamiltonian.

$$\mathcal{H} = \mathcal{H}_{zeeman} + \mathcal{H}_{hyperfine} = g\beta HS_z/\hbar + hA(I_z/\hbar)(S_z/h)$$

Where A is the energy of the hyperfine interaction, I_z is the spin of the nucleus. Considering the Zeeman interaction and hyperfine splitting, the energy of the electron is

$$E = g\beta H m_s + hAm_I m_s$$

Selection rules determining the "allowed" electron energy-level transitions state that the change in electron spin $m_s = \pm ½$, and the change in nuclear spin $m_I = 0$. Thus, there are three possible transitions (**Figure 8**, A), and the difference in energy is

$$\Delta E = g\beta H + hAm_I \qquad \textbf{[eq. 2.2]}$$

These three transitions lead to the three-lined EPR spectrum of a nitroxide spin label (**Figure 8**, B), with a splitting T between lines, where $T = hA/g\beta$. Substituting T into eq. 2.2, and solving for H (or H_{res}, when $\Delta E = h\nu$) yields

$$H_{res} = h\nu/g\beta - m_I T \qquad \textbf{[eq. 2.3]}$$

The following sections will examine the anisotropic nature of g and T.

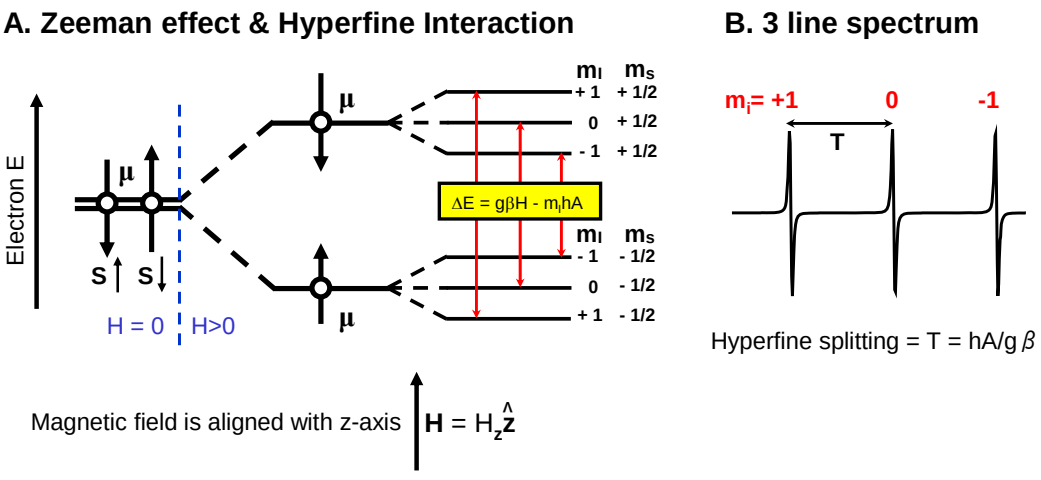

Figure 8 The Hyperfine Interaction.
A: For nitroxide spin labels, energy level splitting from the Zeeman effect and nuclear hyperfine interaction leads to three transitions between electron spin states. B: Three lined spectrum characteristic of nitroxide spin labels.

2.6 EPR is Sensitive to Orientation

In this work, EPR is used to determine the orientation of a spin label's principal axes with respect to an oriented assembly (the actin filament). The first step in this effort is spin-labeling myosin. Strategically labeling myosin has made it possible to achieve rigid coupling between the spin label and peptide backbone. Therefore, we can make the assumption that the behavior of the spin label is characteristic of the peptide backbone. The orientational sensitivity of EPR arises from the anisotropic interaction of the nitroxide group on the spin label with the applied magnetic field **H**. This section examines the effect of orientation on the position and shape of lines in an EPR spectrum.

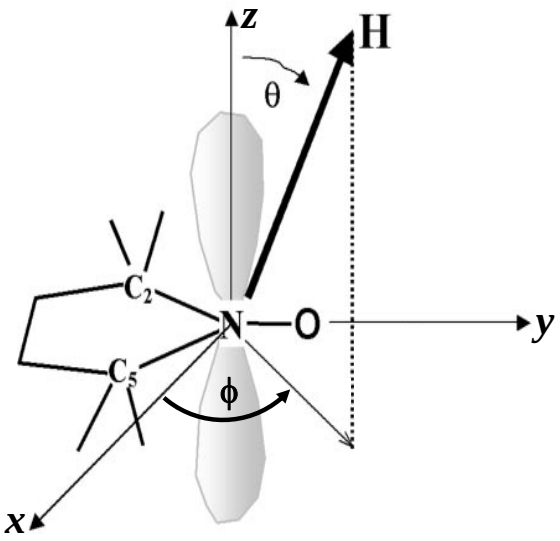

Figure 9 Orientation of the applied magnetic field in the spin label coordinate frame.
The coordinate frame of the spin label is such that the x-axis is aligned with the N-O bond and the z-axis is perpendicular to the aromatic ring (approximately parallel with the unpaired electron's π-orbital). The vector representing the applied field **H** is defined by θ and ϕ. Adapted from (22).